Appl. Phys. A (2015) 119:1197–1201
DOI 10.1007/s00339-015-9177-1

Applied Physics A
Materials Science & Processing

RAPID COMMUNICATION

Growth of vertically aligned ZnO nanorods on Teflon as a novel substrate for low-power flexible light sensors

O. F. Farhat[1] · M. M. Halim[1] · M. J. Abdullah[1] · M. K. M. Ali[1] · Naser M. Ahmed[1] · Nageh K. Allam[2]

Received: 15 January 2015 / Accepted: 8 April 2015 / Published online: 17 April 2015

Abstract In this work, vertically aligned zinc oxide (ZnO) nanorods were successfully grown by a wet chemical bath deposition method on a ZnO seed-layer-coated Teflon substrate at room temperature. The strong and sharp (0 0 2) peak in the XRD pattern along with the calculated low compressive strain indicated the vertical growth of high-quality crystalline ZnO nanorods along the *z*-axis on the substrate. The field emission scanning electron microscopy images show the ZnO nanorods to have diameters ranging from 34 to 52 nm. Raman analyses revealed a high E_2 (high) peak at 440.23 nm. A flexible ZnO nanorod-based metal–semiconductor–metal UV detector was fabricated. The device showed a sensitivity of 1466. The responsivity (*R*) of the device is 2.265 A/W, which is 20 times higher than that reported for ZnO-based PDs. Under low power illumination (370 nm, 1.5 mW/cm^2), the device showed a relatively fast response and baseline recovery for UV detection. The prototype device shows a simple method for nanorod synthesis and demonstrates the possibility of constructing nanoscale photodetectors for nano-optics applications.

1 Introduction

The mutual advantages of wide direct band gap (3.37 eV), high exciton binding energy (60 meV), and strong room-temperature emission characteristics of ZnO led to numerous in-depth studies to synthesize a variety of ZnO nanostructures [1]. Among these various morphologies, the one-dimensional (1D) ZnO nanorods have recently attracted significant attention due to their unique shape and structure resulting in remarkable optoelectronic, piezoelectric, and magnetic properties. Specifically, the high optical gain of ZnO [2] makes it the material of focus in sensing and optoelectronics applications [3–5].

Flexible sensors are playing an increasingly important role in optoelectronics applications. While the biggest market is currently for glucose sensors used by diabetics, other types of flexible sensors are emerging. IDTechEx forecasts that the market for flexible sensors will have increased by more than $1 billion by 2020 [6]. To this end, several types of flexible polymeric materials, such as polyethylene naphthalate (PEN) and polyethylene terephthalate (PET), are currently considered due to their exceptional corrosion resistance and dielectric properties, low coefficient of friction, high processing temperature between 196 and 260 °C, and low cost among other features [7, 8].

Herein, we report the successful fabrication of vertically aligned ZnO nanorods for the first time on Teflon sheet as a novel substrate with above-mentioned polymer advantages and investigate their applicability as flexible light sensors.

2 Experimental details

The growth of ZnO nanorods on ZnO seed-layer-coated Teflon (PTFE) substrates involved three steps: (1) The PTFE substrates were first cleaned in isopropyl alcohol solution in ultrasonic bath at 60 °C for 15 min, (2) ZnO seed layer was grown on the cleaned PTFE substrates using radio frequency magnetron sputtering system at 200 °C with argon pressure and sputtering power of 5.5 mTorr and 150 W, respectively,

✉ Nageh K. Allam
nageh.allam@aucegypt.edu

[1] Nano-Optoelectronics Research and Technology Laboratory, School of Physics, Universiti Sains Malaysia, 11800 Penang, Malaysia

[2] Energy Materials Laboratory (EML), Physics Department, School of Sciences and Engineering, The American University in Cairo, New Cairo 11835, Egypt

resulting in a 100-nm-thick ZnO seed layer that has been post-annealed in a furnace at 200 °C for 1 h, (3) the ZnO nanorods were grown on the ZnO seed layer/PTFE substrates using low-temperature chemical bath deposition (CBD) method. In the CBD growth, 0.05 M zinc nitrate hexahydrate ($Zn(NO_3)_6H_2O$) and an equal molar concentration of hexamethylenetetramine ($C_6H_{12}N_4$) were dissolved separately in deionized water at 80 °C. The two solutions were combined in a beaker, and the substrates were placed vertically inside the beaker, which was placed inside an oven at 95 °C for 3 h. Finally, the samples were rinsed by DI water. The surface morphology of the grown ZnO nanorods was investigated by field emission scanning electron microscope (FESEM) (model FEI/Nova NanoSEM450). The structure and growth orientation of ZnO nanorods were determined by X-ray diffraction (XRD) (PANalytical X'Pert PROMRDPW3040). Raman spectroscopy (JobinYvon HR800UV) was used to investigate the structure of the ZnO nanorods at room temperature with an argon ion laser (514.5 nm) source, incident laser power of 20 mW and a system resolution of 1 cm^{-1}. The MSM photodiode consists of two interdigitated electrodes with four fingers each. Each finger is 230 μm wide and 3.3 mm long, and the spacing between each finger is 400 μm. Palladium (Pd) contacts were deposited by vacuum thermal evaporation using a metal mask based on the pattern of the contact structure. The device was then annealed at 425 °C for 5 min under N_2 atmosphere. The *I–V* characteristics were measured by a KEITHLEY 2400 SCS semiconductor characterization system. The wavelength of the used UV light is 370 nm.

3 Results and discussion

3.1 Characterization of the ZnO nanorods

Figure 1a, b shows the typical FESEM images of the ZnO nanorod arrays grown on the ZnO seed layer/PTFE substrates. High-density ZnO nanorods with diameters ranging from ~34 to 51 nm were successfully obtained. No delamination was observed, which highlights the importance of the ZnO seed layer. Figure 1c shows the EDX spectrum of the grown ZnO nanorods, showing peaks for both Zn and O atoms with approximately similar atomic percentage (Zn/O = 54.4:45.6), which may indicate the synthesis of vacancy-free ZnO nanorods [9]. Also, note that the obtained ZnO nanorods are nanograined and contain well-developed free surfaces as well as grain boundaries. It was reported that the grain boundaries are the intrinsic origin of ferromagnetism in ZnO nanostructures [7, 8, 10]. The small diameter and small grain size of the ZnO nanorods are considered new benchmarks that may be useful for photovoltaic, photocatalysis, and spintronics applications [7, 8, 10].

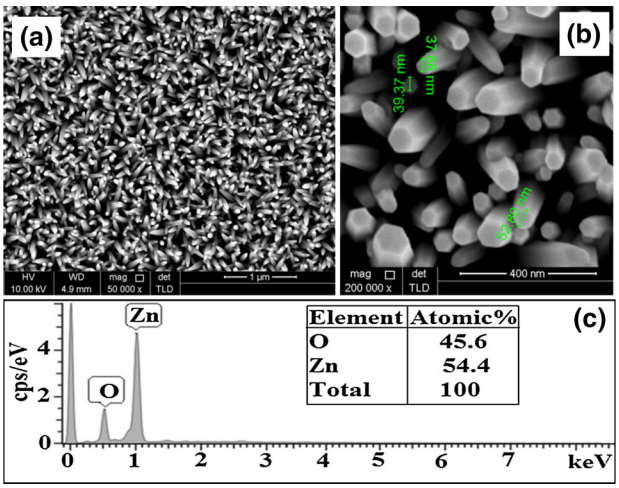

Fig. 1 **a**, **b** FESEM images and **c** EDX spectrum of the ZnO nanorods grown on ZnO seed layer/PTFE substrates

The crystal quality and orientation of the grown ZnO nanorods on ZnO seed layer/PTFE substrates were analyzed by XRD, Fig. 2. The obtained diffraction peaks can be related to crystalline ZnO with hexagonal wurtzite structure (ICSD01080-0074) [7], except for the four peaks located at 2θ of 37.156, 41.312, 47.383, and 49.115, which can be related to the PTFE substrate. The peak at 2θ = 34.321 can be related to the ZnO structure with (0 0 2) orientation, indicating the growth of nanorods along the *c*-axis [11]. The narrow full width at half maximum (FWHM) of the peak indicates the good crystallinity of the grown nanorods.

The strain (ε_c) of the ZnO nanorods synthesized on the ZnO seed layer/PTFE substrates along the *c*-axis was calculated using the following equation [12]:

$$\varepsilon_c = \frac{c - c_0}{c_0} \times 100 \quad (1)$$

where *c* and c_0 are the lattice constant of the ZnO nanorods obtained from the XRD data and the standard lattice constant for unstained ZnO (ICSD 01-080-0074), respectively.

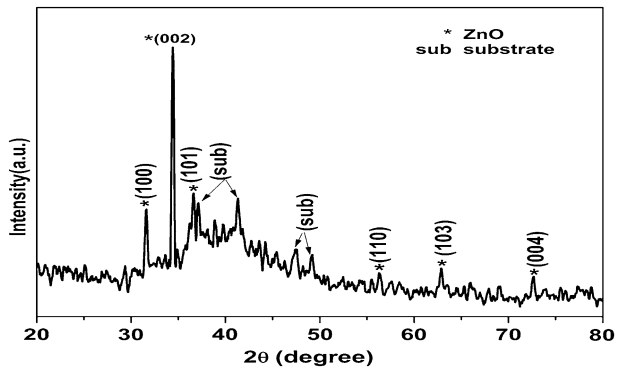

Fig. 2 XRD pattern of the ZnO nanorods grown on ZnO seed layer/PTFE substrate

The calculated strain was −0.03831 %. The negative value indicates the compressive strain for the ZnO nanorods. This low compressive strain confirms the high-quality crystal structure of ZnO nanorods. The average crystallite size (D) of the ZnO nanorods is calculated using the Scherer equation for the (0 0 2) peak [13]:

$$D = \frac{0.90\lambda}{\beta \cos\theta} \tag{2}$$

where λ is the wavelength of incident X-ray and β is the FWHM in radians. The calculated average crystallite size of the ZnO nanorods on the PTFE substrate was determined to be 44.14 nm.

Figure 3 shows the room-temperature Raman spectra of the ZnO nanorod arrays grown on PTFE substrate. The peaks appeared at 385.86 and 734.12 cm^{-1} can be assigned to the scattering from the PTFE substrate. The observed peak of E_2 (high) at 440.23 cm^{-1} is related to ZnO nanorods. The downshift of E_2 (high) mode of ZnO nanorod arrays compared to that usually seen at 437 cm^{-1} for strain-free ZnO bulk crystal [14, 15] indicates a tensile strain in the aligned ZnO nanorod films grown on PTFE substrate. Consequently, the Raman scattering results are in a good agreement with the XRD results.

3.2 Characteristics of the ZnO nanorod MSM UV photodetector

Figure 4a shows a picture of the fabricated metal–semiconductor–metal (Pd–ZnO–Pd) photodetector. The current–voltage (I–V) characteristics of the photodetector under dark and UV illumination (370 nm, 1.5 mW) conditions at room temperature under applied bias from −5 to 5 V are shown in Fig. 4b. Under a bias of +5 V, the dark current of the ZnO nanorod photodetector was 2.2 μA, while the obtained photocurrent was 28.3 μA. The low dark current helps to enhance the signal-to-noise ratio (S/N) of the detector as the shot noise is proportional to the

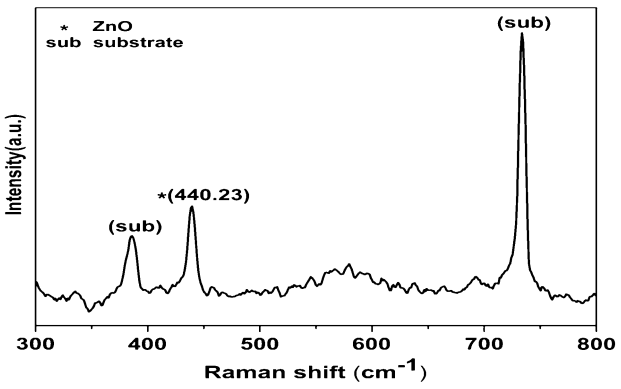

Fig. 3 Raman spectra of the ZnO nanorods grown on ZnO seed layer/PTFE substrate

dark current. The responsivity (R) of the photodetector at +5 V was determined using the following equation [16]:

$$R = \frac{I_{ph}}{AP_{opt}} \tag{3}$$

where I_{ph} is the photocurrent, A is the illuminated area, and P_{opt} is the incident optical power. The obtained R in this study was 2.265 A/W, more than 20 times higher than those reported for ZnO nanorod-based photodetectors [17]. This high R can be attributed to the effect of the ZnO seed layer. R can also be defined as [18].

$$R = \eta \frac{q}{hc} G \tag{4}$$

where η is the external quantum efficiency, q is the electron charge, λ is the incident light wavelength, G is the photoconductive gain, h is the Planck's constant, and c is the speed of light. According to Eq. 4, the quantum efficiency is not more than 1, implying that the high responsivity of the photodetector originated from high internal gain [18]. The large photocurrent density as well as responsivity can be ascribed to more carriers collected under illumination in the ZnO nanorod films. The response in the UV region was due to the band-to-band transitions in the ZnO nanorod films. The photosensitivity (S) of the fabricated UV photodetector was calculated via the following relationship [19]:

$$S = \frac{I_{ph} - I_{dark}}{I_{dark}} \times 100 \tag{5}$$

where I_{ph} is the photocurrent and I_{dark} is the dark current.

The obtained photosensitivity of the fabricated UV photodetector at same applied bias voltage (5 V) was 1466 %.

As the photoconductive response is another key figure of merit for a photodetector, the optical response was studied using dynamic response time measurements via exposing the device to a pulse at 370-nm UV light (1.5 mW) illumination at applied bias of 5 V to test the reversibility of the photodetector. Figure 4c shows the obtained photoresponse as a function of time, while the UV light was switched on and off at constant durations. Note that the response time is the time needed to reach $1 - (1/e)$ of the maximum photocurrent, while the recovery time is the time needed to drop the photocurrent to $1/e$ of its maximum value. In this work, the measured current rapidly increased upon exposure to UV light and then decreased under dark conditions. Table 1 shows the values of the measured rise (6.7 s at 5 V) and decay (9.3 s at 5 V) times of the (Pd–ZnO NRs–Pd) UV detector. These values can be considered as ultra-fast response and recovery times and indicate the high quality of the fabricated ZnO nanorods [20]. While the observed short rise time can be related to the reduced carrier transit times in low-diameter ZnO, the fast recovery time can be attributed

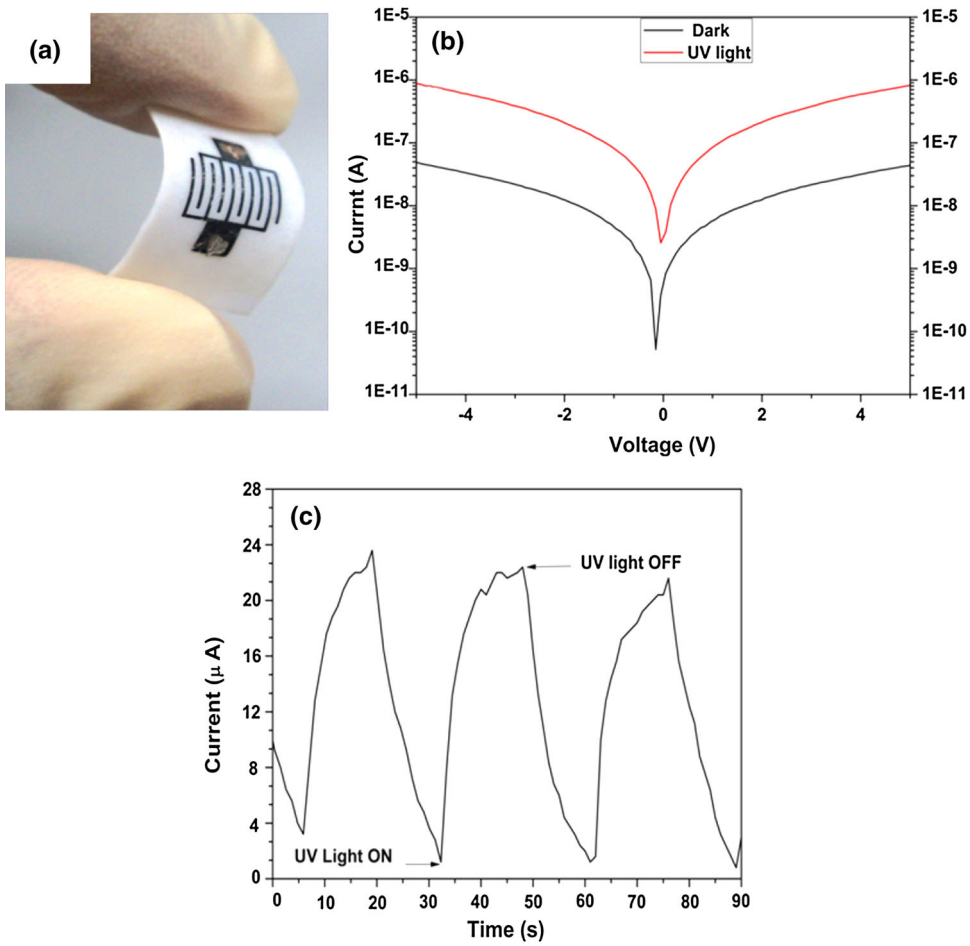

Fig. 4 **a** A picture of the fabricated metal–semiconductor–metal (Pd–ZnO–Pd) photodetector, **b** the *I*–*V* characteristics, and **c** the photodynamic response at 5 V of the ZnO nanorod MSM photodetector under dark and under UV illumination (370 nm, 1.5 mW)

to the rapid electron–hole pair recombination process upon switching the UV light off [20]. Also it has been reported [21] that the current rise in the ZnO nanostructures under UV exposure can be attributed to the increase in the charge carrier density caused by the introduction of additional photogenerated electrons, together with the lowered barrier height caused by photodesorption of negatively charged surface oxygen. However, the current decay in dark condition can be attributed to chemisorptions of oxygen on the surface of ZnO nanostructures that capture electrons from the ZnO nanorods [21].

4 Conclusions

Vertically aligned ZnO nanorods have been synthesized using wet chemical bath deposition (CBD) method on ZnO seed layer/PTFE substrates at room temperature. The sharp and low full width at half maximum intensity of the (0 0 2) peak in the XRD pattern indicated that the ZnO nanorods were vertically grown along the *c*-axis on the substrate and exhibited a high-quality single-crystalline structure. FESEM examination demonstrated the formation of nanorods with diameters ranging from 37.88 to 52.80 nm. In addition, the low compressive strain (−0.03831 %) confirmed the high-quality crystal structure of the ZnO nanorods. The use of Teflon, which has excellent chemical, physical, and mechanical characteristics, as a substrate to grow ZnO nanorods enables the successful fabrication of flexible sensors. The fabricated Pd–ZnO NRs–Pd photodetector showed a photosensitivity of 1466. The responsivity (*R*) was found to be 2.265 A/W, which is 20 times higher than that reported for ZnO-based PDs. Under low power illumination (370 nm, 1.5 mW/cm^2), the device showed a response time of 6.7 s and a baseline recovery time of 9.3 s for UV detection.

Table 1 Photoelectrical parameters of the Pd–ZnO–Pd UV photodetector

Rise time (s)	Decay time (s)	Photosensitivity (%)	Responsivity (A/W)
6.7	9.3	1466	2.265

References

1. A. Kołodziejczak-Radzimska, T. Jesionowski, Zinc oxide—from synthesis to application: a review. Materials **7**, 2833–2881 (2014)
2. Y. Chen, D. Bagnall, H.K. Park, K. Hiraga, Z. Zhu, T. Yao, Plasma assisted molecular beam epitaxy of ZnO on c-plane sapphire: growth and characterization. J. Appl. Phys. **84**, 3912–3918 (1989)
3. A. Singh, D. Kumar, P.K. Khanna, A. Kumar, M. Kumar, M. Kumar, Thin Solid Films **519**, 5826 (2011)
4. N. Samir, D.S. Eissa, N.K. Allam, Self-assembled growth of vertically aligned ZnO nanorods for light sensing applications. Mater. Lett. **137**, 45–48 (2014)
5. F. Xu, M. Dai, Y.N. Lu, L.T. Sun, Hierarchical ZnO nanowire–nanosheet architectures for high power conversion efficiency in dye-sensitized solar cells. J. Phys. Chem. C **114**, 2776 (2010)
6. G. Chansin, printed and flexible sensors 2014–2024: technologies, players, forecasts. IDTechEx, http://www.idtechex.com/research/reports/printed-and-flexible-sensors-2014-2024-technologies-players-forecasts-000367.asp
7. R. Shabannia, H. Abu Hassan, Controllable vertically aligned ZnO nanorods on flexible polyethylene naphthalate (PEN) substrate using chemical bath deposition synthesis. Appl. Phys. A **114**, 579–584 (2014)
8. E.L. Bedia, S. Murakami, T. Kitade, S. Kohjiya, Structural development and mechanical properties of polyethylene naphthalate/polyethylene terephthalate blends during uniaxial drawing. Polymer **42**, 7299–7305 (2001)
9. G. Shen, Y. Bando, C.-J. Lee, Growth of self-organized hierarchical ZnO nanoarchitectures by a simple In/In2S3 controlled thermal evaporation process. J. Phys. Chem. B **109**, 10779–10785 (2005)
10. S. Xu, N. Adiga, S. Ba, T. Dasgupta, C.F.J. Wu, Z.L. Wang, Optimizing, improving the growth quality of ZnO nanowire arrays guided by statistical design of experiments. ACS Nano **3**, 1803–1812 (2009)
11. O.F. Farhat, M.M. Halim, M.J. Abdullah, M.K.M. Ali, N.K. Allam, Morphological and structural characterization of single-crystal ZnO nanorod arrays on flexible and non-flexible substrates. Beilstein J. Nanotechnol. **6**, 720–725 (2015)
12. J.J. Hassan, Z. Hassan, H. Abu-Hassan, High-quality vertically aligned ZnO nanorods synthesized by microwave-assisted CBD with ZnO–PVA complex seed layer on Si substrates. J. Alloys Compd. **509**, 6711–6719 (2011)
13. A. Goux, T. Pauporté, J. Chivot, D. Lincot, Temperature effects on ZnO electrodeposition. Electrochim. Acta **50**, 2239–2248 (2005)
14. X. Zhu, H. Wu, Z. Yuan, J. Kong, W. Shen, Multiphonon resonant Raman scattering in N-doped ZnO. J. Raman Spect. **40**, 2155–2161 (2009)
15. Shuxia Guo, Du Zuliang, Shuxi Dai, Analysis of Raman modes in Mn-doped ZnO nanocrystals. Phys. Status Solidi B **246**, 2329–2332 (2009)
16. L. Li, P. Wu, X. Fang, T. Zhai, L. Dai, M. Liao, Y. Koide, H. Wang, Y. Bando, D. Golberg, Single-crystalline CDS nanobelts for excellent field-emitters and ultrahigh quantum-efficiency photodetectors. Adv. Mater. **22**, 3161–3165 (2010)
17. N.K. Hassan, M.R. Hashim, N.K. Allam, Low power UV photodetection characteristics of cross-linked ZnO nanorods/nanotetrapods grown on silicon chip. Sens. Actuators, A **192**, 124–129 (2013)
18. L.W. Ji, S.M. Peng, Y.K. Su, S.J. Young, C.Z. Wu, W.B. Cheng, Ultraviolet photodetectors based on selectively grown ZnO nanorod arrays. Appl. Phys. Lett. **94**, 203106 (2009)
19. B. Yuan, X.J. Zheng, Y.Q. Chen, B. Yang, T. Zhang, High photosensitivity and low dark current of photoconductive semiconductor switch based on ZnO single nanobelt. Solid State Electron. **55**, 49–53 (2011)
20. J.J. Hassan, M.A. Mahdi, S.J. Kasim, N.M. Ahmed, H. Abu Hassan, Z. Hassan, High sensitivity and fast response and recovery times in a ZnO nanorod array/p-Si self-powered ultraviolet detector. Appl. Phys. Lett. **101**, 261108 (2012)
21. S.K. Mishra, S. Bayan, Defect-dominated optical emission and enhanced ultraviolet photoconductivity properties of ZnO nanorods synthesized by simple and catalyst-free approach. Appl. Phys. A **115**, 1193 (2014)